

PCCP

Accepted Manuscript



This is an *Accepted Manuscript*, which has been through the Royal Society of Chemistry peer review process and has been accepted for publication.

Accepted Manuscripts are published online shortly after acceptance, before technical editing, formatting and proof reading. Using this free service, authors can make their results available to the community, in citable form, before we publish the edited article. We will replace this *Accepted Manuscript* with the edited and formatted *Advance Article* as soon as it is available.

You can find more information about *Accepted Manuscripts* in the [Information for Authors](#).

Please note that technical editing may introduce minor changes to the text and/or graphics, which may alter content. The journal's standard [Terms & Conditions](#) and the [Ethical guidelines](#) still apply. In no event shall the Royal Society of Chemistry be held responsible for any errors or omissions in this *Accepted Manuscript* or any consequences arising from the use of any information it contains.



Journal Name

ARTICLE

Heterocycle Containing Different Atoms as π -bridge effect on the Performance of Dye-Sensitized Solar Cells

Hailang Jia,^a Xuehai Ju,^b Mingdao Zhang,^a Zemin Ju^a and Hegen Zheng^{*a}

Received 00th January 20xx,
Accepted 00th January 20xx

DOI: 10.1039/x0xx00000x

www.rsc.org/

Two new D- π -A zinc porphyrin dyes with thiophene and furan π -bridges have been synthesized and employed in dye-sensitized solar cells (DSSCs). Here, the triphenylamine (TPA) moiety was used as the electron donor, in addition, the hexylthiophene chromophores were introduced onto the donor groups, which effectively extended the π -conjugation system. Although the two dyes had a similar molecular structure, but there was a significant difference between the optical properties and the photoelectric properties. The EIS analysis suggested that the dye with thiophene π -bridge had a lower charge recombination rate compared to the dye with furan π -bridge. Combined with their light-harvesting ability, thus the PCE of dye JP-S was higher than that of the dye JP-O. The JP-S based DSSCs showed the PCE of 5.84%, whereas, the PCE of JP-O based DSSCs was 4.68%. Moreover, the dye TTR1 was used as a cosensitizer, it could make up for the poor absorption of porphyrin dyes in the 480-600 nm range and reduce the charge recombination. The JP-S+TTR1 based DSSCs showed a higher PCE of 6.71%, the J_{sc} and V_{oc} of the device were both increased by this strategy.

Introduction

During the past two decades, dye-sensitized solar cells (DSSCs) have attracted widespread interest as a solar energy conversion technology due to their low-cost fabrication and relatively high performance.^{1,2} Since they were first reported by Grätzel and co-workers in 1991, the power conversion efficiency (PCE) of the device had made breakthrough progress.³ DSSCs, comprising mesoporous metal oxides, sensitizers, redox electrolyte and counter electrode.^{4,5} Among all the components of a DSSC, the sensitizers play the key role in achieving high PCE. Up to now, the DSSCs based on ruthenium-complexes have shown high efficiency of up to 11.9%.^{6,7} Recently, Grätzel and co-workers used Zn porphyrin dye SM315 with the cobalt-based redox electrolyte resulted in DSSCs that showed the highest PCE of 13%.⁸ Thus, the development of novel and efficient sensitizer is one of the most direct and effective ways to improve the performance of DSSCs.^{9,10}

Commonly, an efficient sensitizer often has a typical donor- π -acceptor (D- π -A) framework, owing to its efficient intra-molecular charge transfer (ICT) property.¹¹⁻¹⁴ In addition, this molecular framework is easy to modify and tailor bandgap energy, thereby broadening the molecular absorption

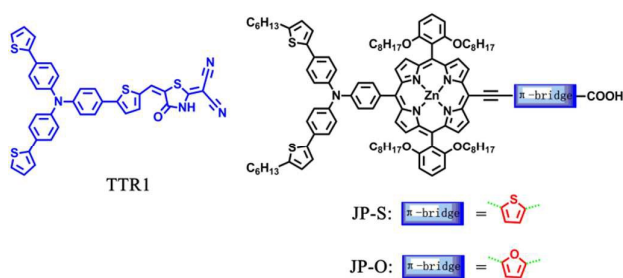
spectrum and increasing the charge carrier mobility. Many efforts have been made to introduce different donors into the dyes to improve the performance, several representative donors including carbazole, triarylamine, diphenylamine, coumarin, phenoxazine, indoline and tetrahydroquinoline.¹⁵⁻²⁰ In addition to the powerful electron-donating effect, the donors can suppress dye aggregation and prevent I_3^- of the electrolyte closing to the TiO_2 surface for their steric effect.^{21,22} The π -bridge play a crucial role in D- π -A framework, it can extend the length of the π -conjugated system, make the absorption range of dyes redshift to the visible and the infrared regions, and ensure the electrons move from donor to acceptor successfully.²³⁻²⁶ Nonetheless, the research on π -bridges is not too much, the typical π -bridges such as cyclohexene, biphenyl, oligothiophene, anthracene, thiazole, fluorene and benzothiadiazole.²⁷⁻³⁰ Different π -bridge will have great influence on the performance of the device, even if only change an atom in the π -bridge. Such as Wong et al. used electron-defect pyrimidine instead of cyclohexene as π -bridge to synthesize dye OHexDPTP, it was red-shifted by 46 nm compared to the parent dye M-TP, and the PCE of the OHexDPTP based-device reached 7.64% which was almost 1.5 times as many as the M-TP based-device.³¹ Thus, the π -bridge should be selected carefully after considering its effect on the performance of DSSCs.

Heterocycles and their derivatives are often used as π -bridges in the design of sensitizer due to their excellent conjugate structures.^{32,33} In our previous work, we synthesized a series of new zinc porphyrin dyes, which adopted heterocycle as π -bridge.³⁴ This strategy not only extended the length of the π -conjugated system, but also suppressed dye aggregation by adjusting the arrangement of dye molecules. In

^a State Key Laboratory of Coordination Chemistry, School of Chemistry and Chemical Engineering, Collaborative Innovation Center of Advanced Microstructures, Nanjing University, Nanjing 210093, P. R. China, E-mail: zhenghg@nju.edu.cn. Fax: 86-25-83314502.

^b School of Chemical Engineering, Nanjing University of Science and Technology, Nanjing 210094, P. R. China, E-mail: xhju@mail.njust.edu.cn
Electronic Supplementary Information (ESI) available: synthesis details and characterization data; Details for all physical characterizations. See DOI: 10.1039/x0xx00000x

this paper, two heterocycles (thiophene and furan) were used as the π -bridges in DSSC. With the purpose of comparing the two different π -bridges, two dyes (JP-S and JP-O) differing only in π -bridge were prepared. Interestingly, we found the two dyes had clearly different optical properties and photovoltaic performance. In addition, the cosensitizer has been widely used for making up for the poor absorption region of the main dye.^{10,35,36} Here, we used triphenylamine dye TTR1 as the cosensitizer, whose maximum absorption peak lay at 535 nm.³⁷ It could make up for the poor absorption of porphyrin dyes in the 480-600 nm range and reduce the charge recombination by occupying the voids between the main dyes. This work aimed to demonstrate how the variation of the π -bridge (thiophene, furan) impacted the PCE of the two dyes based-device.



Schem 1 Chemical structures of JP-S, JP-O and cosensitizer TTR1

Experimental

Synthesis of dyes

The chemical structures of JP-S, JP-O and cosensitizer TTR1 were shown in Scheme 1, and the synthetic route was depicted in Scheme S1. The dye JP-S and TTR1 was synthesized according to the ref. 34 and ref. 37, respectively.

Fabrication of DSSCs

The DSSCs were fabricated using a double-layered photoanode made of mesoporous TiO₂. The photoanode (active area 0.16 cm²) was prepared by screen printing the TiO₂ paste on fluorine-doped tin oxide (FTO) glass plates (15 Ω / square). For the preparation of a DSSC, FTO glass plates were cleaned in a detergent solution using an ultrasonic bath for 30 min for two times and then rinsed with water and ethanol. Then, the plates were immersed in 40 mM TiCl₄ (aqueous) at 70 $^{\circ}$ C for 30 min and washed with water and ethanol. The TiO₂ pastes consisted of 8 μ m thick film (particle size, 20 nm, pore size 32 nm) and 6 μ m thick layer of scattering particles (400 nm diameter). The TiO₂ films were performed with a programmed procedure: (1) heating at 80 $^{\circ}$ C for 15 min; (2) heating at 135 $^{\circ}$ C for 10 min; (3) heating at 325 $^{\circ}$ C for 30 min; (4) heating at 375 $^{\circ}$ C for 5 min; (5) heating at 450 $^{\circ}$ C for 15 min, and (6) heating at 500 $^{\circ}$ C for 15 min. Then the films were treated again with TiCl₄ at 70 $^{\circ}$ C for 30 min and sintered at 500 $^{\circ}$ C for 30 min. After cooling down to 80 $^{\circ}$ C, they were immersed into 0.2 mM dye (JP-S and JP-O) solution in THF/Ethanol (1:4). The photoanodes underwent dipping for 18 h at room temperature to complete the loading with

sensitizer. For cosensitization, the porphyrin-sensitized films were washed with ethanol and dried, then immersed in 0.3 mM cosensitizer (TTR1) solution in DCM for 1.5 h at room temperature. The Pt counter electrodes were prepared on spin-coating drops of H₂PtCl₆ solution onto FTO glass and heating at 385 $^{\circ}$ C for 20 min. The photoanodes and the Pt counter electrode were sealed with a Surlyn film (25 μ m) at 110 $^{\circ}$ C. The electrolyte was introduced to the cells via pre-drilled holes in the counter electrode, the hole was sealed with a Surlyn film and a thin glass (0.1 mm thickness) cover by heating. The electrolyte was composed of 0.6 M 1-butyl-3-methylimidazolium iodide (BMII), 30 mM I₂, 50 mM LiI, 0.5 M tert-butylpyridine and 0.1 M guanidiniumthiocyanate (GuNCS) in a solvent mixture of acetonitrile and valeronitrile (85:15, V/V).

Device characterization

The photocurrent-voltage (*J-V*) curves of the devices were measured on a Keithley 2400 source meter under an irradiance of 100 mW cm⁻² at the surface of a testing cell by a xenon light source (Oriol). The incident photo-to-electron conversion efficiency (IPCE) spectra of the devices were measured by a DC method. The light source was a 300 W xenon lamp (Oriol 6258) coupled with a flux controller to improve the stability of the irradiance. The single wavelength was selected by a monochromator (Cornerstone 260 Oriol74125). Light intensity was measured by a NREL traceable Si detector (Oriol 71030NS) and the short circuit currents of the devices were measured by an optical power meter (Oriol 70310).

Theoretical calculations

Density function theory (DFT) calculations were performed at the DFT-B3LYP/LanL2MB level with Gaussian 09 suite of programs.

UV-Vis absorption spectra, photoluminescence, FTIR spectra and electrochemical properties

UV-vis absorption spectra were recorded on a Shimadzu UV-3600 spectrometer. For the absorption spectra of the dyes on TiO₂, a blank TiO₂ film was used for baseline correction before testing. Fluorescence spectra were recorded on a Perkin Elmer LS55 spectrophotometer. FTIR spectra were recorded on a Vector22 spectrometer. The fluorescence lifetimes of the dyes were measured on a FLS920 spectrometer. Quasi-reversible oxidation and reduction waves were recorded on a Chenhua CHI660D model Electrochemical Workstation (Shanghai). Electrochemical Impedance Spectroscopy was studied using a Chenhua CHI660I model Electrochemical Workstation (Shanghai).

Results and discussion

Optical properties

Fig. 1 showed the UV-Vis absorption spectra of JP-S, JP-O and cosensitizer TTR1 in DCM, and the corresponding data were collected in Table 1. The dye JP-S and JP-O exhibited typical zinc porphyrin absorption characteristics. The two dyes all exhibited high molar extinction coefficients in the high energy

Table 1 Optical and electrochemical properties of dyes

| Dye | ^a λ_{\max}/nm ($\epsilon \times 10^5 \text{ M}^{-1} \text{ cm}^{-1}$) | ^b λ_{\max}/nm | ^c HOMO/V (vs. NHE) | ^d $E_{0,0}$ /eV | ^e LUMO/V (vs. NHE) |
|------|--|---|----------------------------------|-------------------------------|----------------------------------|
| JP-S | 449(2.89) 568(0.26) 622(0.46) | 659 | 1.09 | 2.02 | -0.93 |
| JP-O | 443(2.79) 565(0.17) 618(0.26) | 643 | 1.12 | 2.06 | -0.94 |

^aAbsorption maximum in DCM solution ($1 \times 10^{-6} \text{ M}$), ^bemission maximum in DCM solution ($1 \times 10^{-6} \text{ M}$), ^cHOMO potentials corresponding to the ground state oxidation potentials (the error number is $\pm 0.02 \text{ V}$), ^d $E_{0,0}$ was estimated from the intercept of the normalized absorption and emission spectra, ^eLUMO was calculated by the formula: $\text{LUMO} = \text{HOMO} - E_{0,0}$.

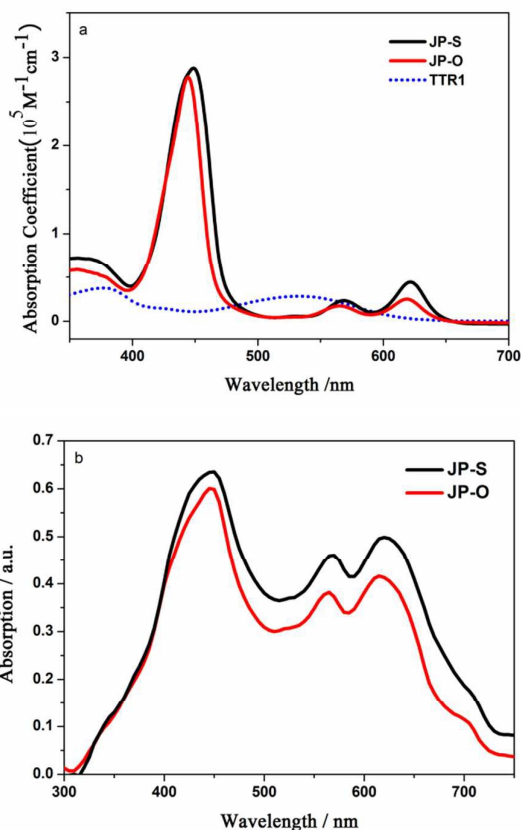


Fig. 1 (a) UV-Vis absorption spectra of JP-S, JP-O and TTR1 in DCM (b) Absorption spectra of JP-S and JP-O anchoring on the $14 \mu\text{m}$ porous TiO_2 nanoparticle film.

absorption region, the dye JP-S reached $2.89 \times 10^5 \text{ M}^{-1} \text{ cm}^{-1}$ at 449 nm , and the dye JP-O reached $2.79 \times 10^5 \text{ M}^{-1} \text{ cm}^{-1}$ at 443 nm . The absorption spectrum of JP-S was red-shifted compared with JP-O, this result suggested that the dye JP-S may had a better light-harvesting ability. The emission spectra of the two dyes were also investigated (Fig. S1), their maxima lay at 659 nm and 643 nm , respectively. It is consistent with the trend of the absorption spectra of the two dyes. In the low energy absorption region, the absorption spectrum of JP-S was higher and broader than that of JP-O. We further investigated the UV-Vis absorption spectra of the two dyes anchoring on $14 \mu\text{m}$ porous TiO_2 nanoparticle films (Fig. 1b). The TiO_2 films consisted of $8 \mu\text{m}$ thick film (particle size, 20 nm , pore size 32

nm) and $6 \mu\text{m}$ thick layer of scattering particles (400 nm diameter).^{8,15} The absorption spectra of the two dyes were all broadened, especially for dye JP-S, it showed significant enhancement compared with dye JP-O at the low energy absorption region. Moreover, the triphenylamine dye TTR1 was used as the cosensitizer, Fig. 1a showed the maximum absorption peak of cosensitizer TTR1 lay at 535 nm . The result indicated that the dye TTR1 can make up for the poor absorption of dye JP-S and JP-O in the $480\text{--}600 \text{ nm}$ range.

Electrochemical studies

Electrochemical properties of dyes were investigated by cyclic voltammetry (Fig. 2), and the corresponding data were collected in Table 1. The ground state oxidation potentials of dye JP-S and JP-O corresponding to the HOMO level energy, are 1.09 and 1.12 V , respectively, vs a normal hydrogen electrode (NHE). The HOMO level of JP-S is cathodically shifted by 30 mV relative to JP-O, which suggests that the dye JP-S is more likely to be oxidized. The values are all more positive than the redox potential of the I^-/I_3^- redox couple (0.4 V vs. NHE), indicating an effective regeneration of the oxidized state. The zero-zero excitation energies ($E_{0,0}$) were estimated from the intercept of the normalized absorption and emission spectra (Fig. S2). The $E_{0,0}$ values of JP-S and JP-O are 2.02 and 2.06 eV , respectively. The excited oxidation potentials corresponding to the LUMO levels, calculated from E_{HOMO} to $E_{0,0}$, are -0.93 and -0.94 V , respectively. They are all more negative than the Fermi level of TiO_2 (-0.5 V vs. NHE), which indicate that the electron from the excited dye can inject into the conduction band of TiO_2 .³⁸

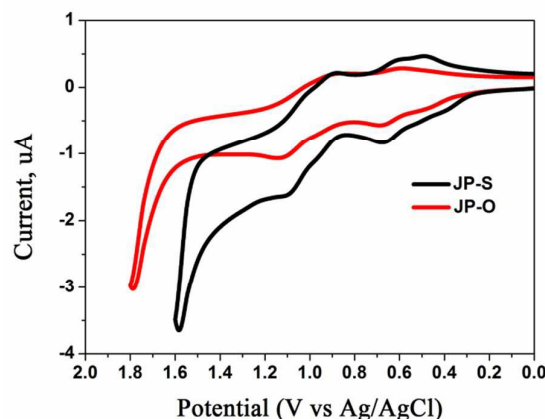


Fig. 2 Cyclic voltammogram of JP-S and JP-O in DCM (0.1 M TBAPF₆, glassy carbon electrode as working electrode, Pt as counter electrode, Ag/Ag^+ as reference electrode, scan rate: 100 mV s^{-1})

Theoretical Calculations

In order to gain more insight into the electronic properties of the two dyes, density function theory (DFT) calculations were performed at the DFT-B3LYP/LanL2MBS level with Gaussian 09 suite of programs. As shown in Fig. S4, the HOMO orbitals of the two dyes were mainly delocalized between the donors and the porphyrin macrocycles, and the LUMO orbitals were mainly delocalized between the porphyrin macrocycles and the acceptors. Thus, the electron can easily transfer from HOMO to LUMO and induce electron redistribution from the donor to the anchoring group. The results indicated that the

electron could effectively injection from the LUMO to the conduction band of TiO_2 .³⁹

Table 2 Photovoltaic parameters of the DSSCs obtained from the J - V curves

| Dye | J_{sc} (mA cm^{-2}) | V_{oc} (V) | FF (%) | η (%) |
|------|----------------------------------|--------------|--------|------------|
| JP-S | 12.63 | 0.676 | 68.3 | 5.84 |
| JP-O | 10.32 | 0.661 | 68.6 | 4.68 |

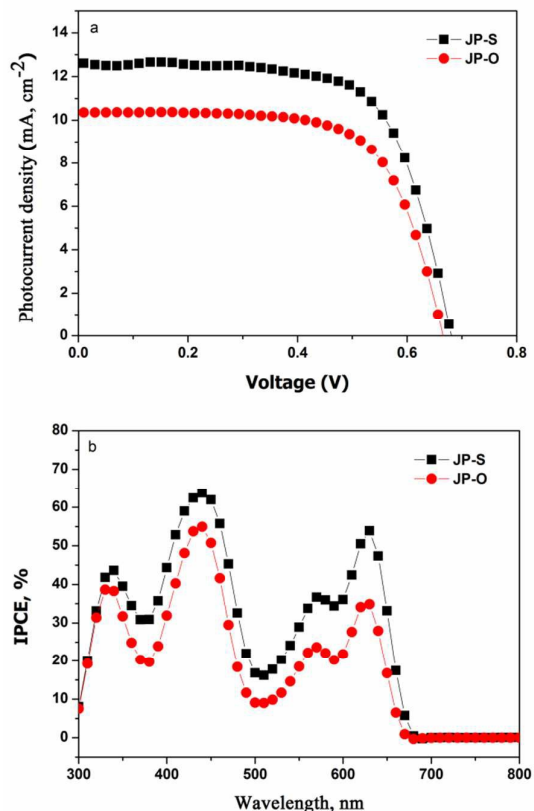


Fig. 3 (a) The J - V curves of DSSCs based on JP-S and JP-O, (b) The IPCE curves of DSSCs based on JP-S and JP-O.

Photovoltaic performance of DSSCs

The current density-voltage (J - V) curves of the DSSCs based on JP-S and JP-O were shown in Fig. 3, and the corresponding parameters were summarized in Table 2. Obviously, the performance of the JP-S based-device was superior to that of the JP-O. The open-circuit photovoltage (V_{oc}) of JP-S is 0.676 V, which is slightly higher than that of JP-O (0.661 V). The difference between the V_{oc} may be due to their different charge recombination resistance (R_{rec}), this will be further investigated by Electrochemical Impedance Spectroscopy (EIS). The short-circuit current density (J_{sc}) of JP-S (12.63 mA cm^{-2}) is higher than that of JP-O (10.32 mA cm^{-2}), it is consistent with the incident photo-to-electron conversion efficiency (IPCE) spectra (Fig. 3b). The IPCE values of JP-S exceed 60% from 420 nm to 455 nm, and achieve 64.8% at 440 nm at the sorlet band. In contrast, the maximum value of JP-O is only 55% at 435 nm. The distribution of the Q band is the same as the Sorlet band, it is clear that the IPCE curve of JP-S is higher and broader than that of JP-O. It is consistent with the trend of UV-Vis

absorption spectra of the two dyes. In order to study clearly about the difference between the IPCE, we will further investigate the time-resolved fluorescence experiments.

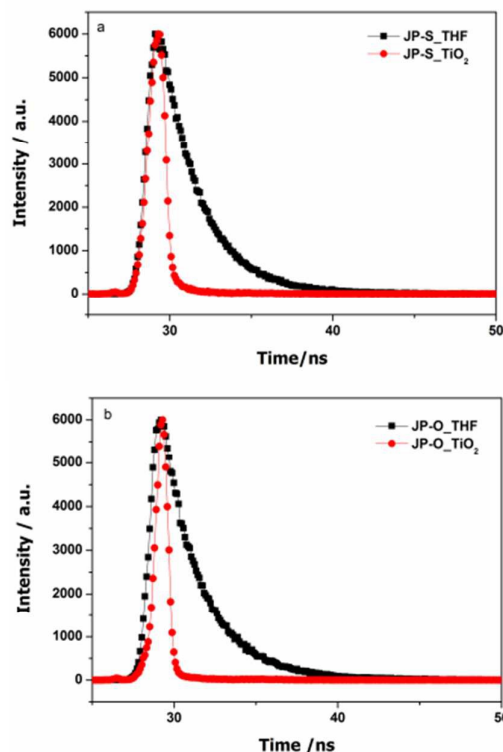


Fig. 4 Fluorescence decay curves of dyes in THF (black line) and dyes adsorbed onto the TiO_2 surface (red line), (a)JP-S, (b)JP-O.

Time-resolved fluorescence analysis

In order to further understand the differences in the dynamics of photoexcited electron injection between the two dyes, we measured the time-resolved fluorescence experiments of the two dyes in THF and adsorbed onto the TiO_2 surface. The fluorescence decay curves were shown in Fig. 4. In THF, the average lifetime values of JP-S and JP-O are 5.75, 3.42 ns, respectively. It is clear that the excited-state lifetime of JP-S in THF is longer than that of JP-O, and they all have enough time to complete the electron injection process. After adsorbed onto the TiO_2 film, the emission of the two dyes were both strongly quenched. But this method cannot detect such rapid electron injection process. Considering the lifetime may belong to the aggregated dyes or attached dyes, and there was no significant difference in the fluorescence kinetics of the two dyes on TiO_2 , so the experiments cannot account for the differences between the IPCE of the two dyes.

Electrochemical impedance spectroscopy analysis

To further investigate the electron recombination effect for the chemical structures of JP-S and JP-O, the Electrochemical Impedance Spectroscopy (EIS) were measured under dark condition. EIS is a powerful tool to investigate the kinetics of photoelectrochemical and electrochemical processes in DSSCs.⁴³ For the Nyquist plot in the dark (Fig. 5a), the larger semicircle corresponds to the electron recombination at the

photoanode/dye/electrolyte interface, and the smaller semicircle corresponds to the electron transport at the Pt/electrolyte. The radius of the larger semicircle represents the charge recombination resistance (R_{rec}). Obviously, the R_{rec} of JP-S is slightly larger than that of JP-O, it is consistent with the V_{oc} of the DSSCs. In addition, from the structures of the two dyes which were optimized by the B3LYP (Fig. S5), we knew that the distance between the triphenylamine nitrogen and the anchoring group was 20.9 Å for JP-S, whereas, the distance for JP-O was 19.8 Å. The result indicated that the furan ring in JP-O obliged the molecular structure to bend with respect to the anchoring group, it would induce back-electron transfer more likely than the dye JP-S, so the V_{oc} and J_{sc} of JP-O was lower than that of JP-S.⁴⁴ From the Bode phase plots of the DSSCs, we can obtain the peak frequency (f) at lower frequency region. The electron lifetime (τ) can be calculated by $\tau=1/(2\pi f)$.⁴⁵⁻⁴⁷ The f of JP-S and JP-O is 17 and 21 Hz, respectively. So the electron lifetime value of JP-S and JP-O is 9.4 and 7.6 ms, respectively. The longer electron lifetime corresponds to lower dark current. It is consistent with the V_{oc} of the DSSCs.

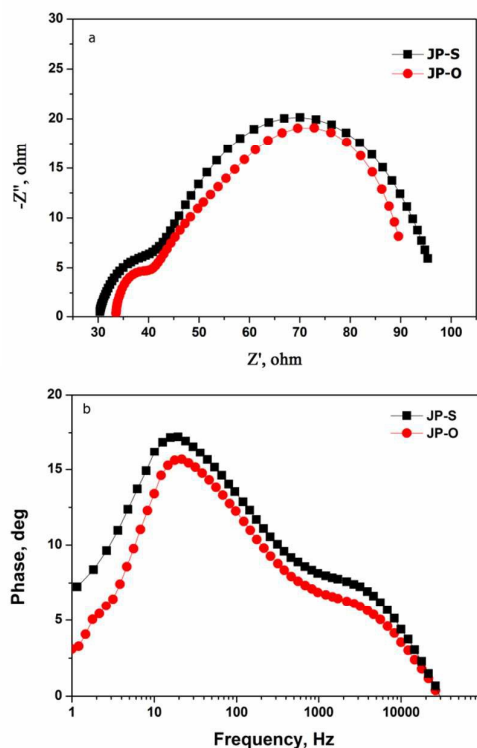


Fig. 5 Nyquist plots (a) and Bode phase plots (b) obtained in the dark of the DSSCs based on JP-S and JP-O.

Coensitization experiments

Recently, the cosensitizer has been widely used to improve the performance of DSSCs, for it can make up for the poor absorption region of the main dye. Here, we took the dye TTR1 as the cosensitizer, the J-V curves of the cosensitized DSSCs were shown in Fig. 6, and the corresponding parameters were summarized in Table 3. Before the cosensitization, the PCE of JP-S and JP-O was 5.84% and 4.68%, respectively. After

cosensitized with TTR1 for 1.5h, their performance were both improved, the PCE of JP-S+TTR1 was 6.71%, and the PCE of JP-O+TTR1 was 5.42%, it was mainly due to the increase of the V_{oc} and J_{sc} . We deduced that the cosensitizer TTR1 can occupy the voids between the main dyes, it was beneficial to suppress the main dye aggregation. Moreover, if the voids between the main dyes were occupied, the I_3^- closed to the TiO_2 surface would become difficult, thereby reducing the electron recombination rate, so the V_{oc} was improved.⁴⁸ We further measured the UV-Vis absorption spectra of the two dyes cosensitized with TTR1 adsorbed onto TiO_2 surface (Fig. S6). Compared with Fig. 1b, the spectrum became higher and broader, especially in the 480-600 nm range. The result is consistent with the IPCE of the cosensitized DSSCs (Fig. 6b). The IPCE values of the two dyes based-device were both increased after coseitized with TTR1, so the J_{sc} of the two dyes were both improved.

Table 3 Photovoltaic parameters of the cosensitized DSSCs obtained from the J-V curves

| Dye | J_{sc} (mA cm ⁻²) | V_{oc} (V) | FF (%) | η (%) |
|------------------------|---------------------------------|--------------|--------|------------|
| ^a TTR1 | 10.35 | 0.717 | 70.0 | 5.20 |
| ^b JP-S+TTR1 | 13.96 | 0.701 | 68.5 | 6.71 |
| ^b JP-O+TTR1 | 11.07 | 0.691 | 70.8 | 5.42 |

^areported in reference 37, ^bthe cosensitized DSSCs were measured under AM 1.5G irradiation, the photoanode was immersed in a solution of the porphyrin (0.2 mM) for 18 h and then immersed in a solution of the TTR1 (0.3 mM) for 1.5 h.

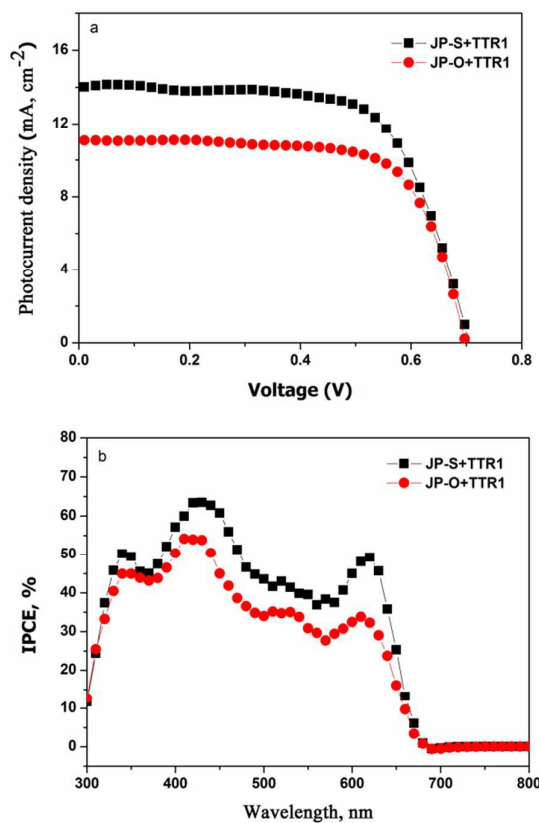


Fig. 6 (a) The J-V curves of DSSCs based on JP-S+TTR1 and JP-O+TTR1, (b) The IPCE curves of DSSCs based on JP-S+TTR1 and JP-O+TTR1.

Conclusions

We synthesized two new D- π -A porphyrin dyes with thiophene and furan π -bridges and applied in dye-sensitized solar cells. Although there was only slight difference between the molecular structures, but this obviously affected their optical properties and photoelectric properties. The absorption spectrum of JP-S was red-shifted compared with JP-O. The EIS analysis suggested that the dye with thiophene π -bridge had a lower charge recombination rate compared to the dye with furan π -bridge. Thus, the PCE of the JP-S based-device (5.84%) was higher than that of JP-O based-device (4.68%). Moreover, we took the triphenylamine dye TTR1 as the cosensitizer, which not only can make up for the poor absorption of the porphyrin dyes in the 480-600 nm range, but also can improve the V_{oc} of DSSCs by suppressing the main dyes aggregation and reducing the charge recombination. The PCE of the JP-S+TTR1 based-device was 6.71%, which increased about 15% compared with the JP-S based-device. This study suggested that the performance of DSSCs could be improved effectively by modulating the π -bridges of the dyes.

Acknowledgements

This work was supported by grants from the National Natural Science Foundation of China (Nos. 21371092; 21401107), National Basic Research Program of China (2010CB923303), Natural Science Foundation of Jiangsu Province, China (No. BK20140986).

Notes and references

- L. L. Li, E. W. G. Diau, *Chem. Soc. Rev.*, 2013, **42**, 291.
- A. Hagfeldt, G. Boschloo, L. Sun, L. Kloo and H. Pettersson, *Chem. Rev.*, 2010, **110**, 6595.
- B. O'Regan, M. Grätzel, *Nature*, 1991, **353**, 737.
- J. D. Roy-Mayhew, I. A. Aksay, *Chem. Rev.*, 2014, **114**, 6323.
- J. Wu, Z. Lan, J. Lin, M. Huang, Y. Huang, L. Fan and G. Luo, *Chem. Rev.*, 2015, **115**, 2136.
- M. K. Nazeeruddin, A. Kay, I. Rodicio, R. Humpbry-Baker, E. Miiller, P. Liska, N. Vlachopoulos and M. Grätzel, *J. Am. Chem. Soc.*, 1993, **115**, 6382.
- Q. J. Yu, Y. H. Wang, Z. H. Yi, N. N. Zu, J. Zhang, M. Zhang and P. Wang, *Acs, Nano.*, 2010, **4**, 6032.
- S. Mathew, A. Yella, P. Gao, R. Humphry-Baker, B. F. E. Curchod, N. Ashari-Astani, I. Tavernelli, U. Rothlisberger, M. K. Nazeeruddin and M. Grätzel, *Nature Chemistry*, 2014, **6**, 242.
- S. Kolemen, O. A. Bozdemir, Y. Cakmak, G. Barin, S. Erten-Ela, M. Marszalek, J.-H. Yum, S. M. Zakeeruddin, M. K. Nazeeruddin, M. Grätzel and E. U. Akkaya, *Chem. Sci.*, 2011, **2**, 949.
- A. Yella, H. W. Lee, H. N. Tsao, C. Yi, A. K. Chandiran, M. K. Nazeeruddin, E. W. G. Diau, C. Y. Yeh, S. M. Zakeeruddin and M. Grätzel, *Science*, 2011, **334**, 629.
- B. G. Kim, K. Chung, J. Kim, *Chem. Eur. J.*, 2013, **19**, 5220.
- M. Urbani, M. Grätzel, M. K. Nazeeruddin and T. Torres, *Chem. Rev.*, 2014, **114**, 12330.
- C.-L. Wang, J.-W. Shiu, Y.-N. Hsiao, P.-S. Chao, E. W.-G. Diau and C.-Y. Lin, *J. Phys. Chem. C*, 2014, **118**, 27801.
- C.-J. Yang, Y. J. Chang, M. Watanabe, Y.-S. Hon and T. J. Chow, *J. Mater. Chem.*, 2012, **22**, 4040.
- J. Yang, P. Ganesan, J. Teuscher, T. Moehl, Y. J. Kim, C. Yi, P. Comte, K. Pei, T. W. Holcombe, M. K. Nazeeruddin, J. Hua, S. M. Zakeeruddin, H. Tian and M. Grätzel, *J. Am. Chem. Soc.*, 2014, **136**, 5722.
- Y. Hua, S. Chang, J. He, C. Zhang, J. Zhao, T. Chen, W.-Y. Wong, W.-K. Wong and X. Zhu, *Chem. Eur. J.*, 2014, **20**, 6300.
- C. Koenigsmann, T. S. Ripolles, B. J. Brennan, C. F. A. Negre, M. Koepf, A. C. Durrell, R. L. Milot, J. A. Torre, R. H. Crabtree, V. S. Batista, G. W. Brudvig, J. Bisquert and C. A. Schmuttenmaer, *Phys. Chem. Chem. Phys.*, 2014, **16**, 16629.
- Y. Wang, B. Chen, W. Wu, X. Li, W. Zhu, H. Tian and Y. Xie, *Angew. Chem. Int. Ed.*, 2014, **53**, 10779.
- K. Hara, Z.-S. Wang, T. Sato, A. Furube, R. Katoh, H. Sugihara, Y. Dan-oh, C. Kasada, A. Shinapo and S. Suga, *J. Phys. Chem. B*, 2005, **109**, 15477.
- D. Kumar, K. R. J. Thomas, C.-P. Lee and K.-C. Ho, *J. Org. Chem.* 2014, **79**, 3159.
- W. I. Hung, Y. Y. Liao, T. H. Lee, Y. C. Ting, J. S. Ni, W. S. Kao, J. T. Lin, T. C. Wei and Y. S. Yen, *Chem. Commun.*, 2015, **51**, 2152.
- M.-E. Ragoussia, T. Torres, *Chem. Commun.*, 2015, **51**, 3957.
- C.-Y. Lin, Y.-C. Wang, S.-J. Hsu, C.-F. Lo and E. W.-G. Diau, *J. Phys. Chem. C*, 2010, **114**, 687.
- Z. Yang, D. Wang, X. Bai, C. Shao and D. Cao, *RSC Adv.*, 2014, **4**, 48750.
- N. Zhou, K. Prabakaran, B. Lee, S. H. Chang, B. Harutyunyan, P. Guo, M. R. Butler, A. Timalina, M. J. Bedzyk, M. A. Ratner, S. Vegiraju, S. Yau, C.-G. Wu, R. P. H. Chang, A. Facchetti, M.-C. Chen and T. J. Marks, *J. Am. Chem. Soc.*, 2015, **137**, 4414.
- J. Lu, S. Liu, H. Li, Y. Shen, J. Xu, Y. Cheng and M. Wang, *J. Mater. Chem. A*, 2014, **2**, 17495.
- S. Jiang, S. Fan, X. Lu, G. Zhou and Z.-S. Wang, *J. Mater. Chem. A*, 2014, **2**, 17153.
- C.-H. Siu, L. T. L. Lee, P.-Y. Ho, P. Majumdar, C.-L. Ho, T. Chen, J. Zhao, H. Lie and W.-Y. Wong, *J. Mater. Chem. C*, 2014, **2**, 7086.
- M. Li, L. Kou, L. Diau, Q. Zhang, Z. Li, Q. Wu, W. Lu and D. Pan, *J. Phys. Chem. A*, 2015, **119**, 3299.
- A. Baheti, K. R. J. Thomas, C.-P. Lee, C.-T. Li and K.-C. Ho, *J. Mater. Chem. A*, 2014, **2**, 5766.
- L.-Y. Lin, C.-H. Tsai, K.-T. Wong, T.-W. Huang, C.-C. Wu, S.-H. Chou, F. Lin, S.-H. Chen and A.-I. Tsai, *J. Mater. Chem.*, 2011, **21**, 5950.
- G. Marotta, M. A. Reddy, S. P. Singh, A. Islam, L. Han, F. D. Angelis, M. Pastore and M. Chandrasekharam, *ACS Appl. Mater. Interfaces*, 2013, **5**, 9635.
- S. E. Brown-Xu, M. H. Chisholm, C. B. Durr, T. L. Gustafson and T. F. Spilker, *J. Am. Chem. Soc.*, 2014, **136**, 11428.
- H. L. Jia, Z. M. Ju, H. X. Sun, X. H. Ju, M. D. Zhang, X. F. Zhou and H. G. Zheng, *J. Mater. Chem. A*, 2014, **2**, 20841.
- N. Shibayama, H. Ozawa, M. Abe, Y. Ooyamac and H. Arakawa, *Chem. Commun.*, 2014, **50**, 6398.
- X. Sun, Y. Wang, X. Li, H. Agren, W. Zhu, H. Tian and Y. Xie, *Chem. Commun.*, 2014, **50**, 15609.
- Z. M. Ju, H. L. Jia, X. H. Ju, X. F. Zhou, Z. Q. Shi, H. G. Zheng and M. D. Zhang, *RSC Adv*, 2015, **5**, 3720.
- J. Jeon, Y. C. Park, S. S. Han, W. A. Goddard, Y. S. Lee and H. Kim, *J. Phys. Chem. Lett.*, 2014, **5**, 4285.
- C. Chen, X. Yang, M. Cheng, F. Zhang, J. Zhao and L. Sun, *ACS Appl. Mater. Interfaces*, 2013, **5**, 10960.
- D. Barpuzary, A. S. Patra, J. V. Vaghasiya, B. G. Solanki, S. S. Soni and M. Quresh, *ACS Appl. Mater. Interfaces.*, 2014, **6**, 12629.
- F. M. Jradi, X. Kang, D. O'Neil, G. Pajares, Y. A. Getmanenko, P. Szymanski, T. Parker, M. A. El-Sayed and S. R. Marder, *Chem. Mater.*, 2015, **27**, 2480.
- J. Mao, N. He, Z. Ning, Q. Zhang, F. Guo, L. Chen, W. Wu, J. Hua and H. Tian, *Angew. Chem. Int. Ed.*, 2012, **51**, 9873.

- 43 F. Fabregat-Santiago, J. Bisquerta, G. Garcia-Belmonte, G. Boschloo and A. Hagfeldt, *Solar Energy Materials & Solar Cells*, 2005, **87**, 117.
- 44 W. Ying, J. Yang, M. Wielopolski, T. Moehl, J.-E. Moser, P. Comte, J. Hua, S. M. Zakeeruddin, H. Tian and M. Grätzel, *Chem. Sci.*, 2014, **5**, 206.
- 45 K. Mahmood, H. J. Sung, *J. Mater. Chem. A*, 2014, **2**, 5408.
- 46 X. Qian, Y.-Z. Zhu, W.-Y. Chang, J. Song, B. Pan, L. Lu, H.-H. Gao and J.-Y. Zheng, *ACS Appl. Mater. Interfaces.*, 2015, **7**, 9015.
- 47 K. R. J. Thomas, N. Kapoor, C.-P. Lee, K.-C. Ho, *Chem. Asian J.*, 2012, **7**, 738.
- 48 G. Li, M. Liang, H. Wang, Z. Sun, L. Wang, Z. Wang and S. Xue, *Chem. Mater.*, 2013, **25**, 1713.